# Drift and Diffusion of Free Excitons in Si

M. A. Tamor and J. P. Wolfe
*Physics Department and Materials Research Laboratory, University of Illinois at Urbana-Champaign, Urbana, Illinois 61801*
(Received 24 March 1980)

The drift of free excitons in an applied strain gradient in Si is directly observed for the first time. The exciton luminescence is detected with temporal, spatial, and spectral resolution in order to map the local force field and measure the exciton velocity. An absolute measurement of the momentum relaxation time $\tau$ is made between 1.3 and 20 K and is well explained by acoustic-phonon scattering. Both diffusion and drift regimes are observable, revealing extremely high exciton mobilities.

PACS numbers: 71.35.+z

The mobility of free carriers in Si and Ge has been of great practical interest for several decades. Investigators have used the evolution of current pulses, as in the classic measurements of Haynes and Shockley,[1] and the Hall effect to measure electron and hole drift mobilities from about 30 K to above room temperature.[2-4] It was found that for samples of sufficient purity the carrier mobility was governed by phonon scattering. However, such measurements were complicated by optical-phonon scattering at high temperatures, and by carrier freezout and impurity scattering at lower temperatures. For these reasons, an accurate measurement of the basic acoustic-phonon scattering rate is difficult.

In the present study, a fundamental measurement of the carrier-phonon scattering process has been made over an extended range of low temperatures, using optically excited free excitons. The experiments present a direct determination of the transport properties of free excitons in Si. These bound electron-hole pairs have a binding energy of 14.7 meV and a lifetime of several microseconds. Since excitons are intrinsic states of the pure crystal, the impurity concentration may be minimized to reduce greatly the impurity scattering normally dominant at low temperatures. In addition, a reduction of impurity scattering is expected because the exciton interacts with impurities only through dipole or higher-order forces. The experiments reveal that the mobility of an exciton is very high and its temperature dependence and magnitude are purely characteristic of the acoustic-phonon scattering mechanism.

Since the exciton is electrically neutral it cannot be accelerated by an applied electric field, nor can any drift motion be detected as a current. However, it is known that in the indirect-gap semiconductors Si and Ge, an applied strain reduces the band gap and therefore the total electron-hole pair energy. This property has been exploited previously to confine excitons and electron-hole droplets spatially to a region of maximum strain.[5,6] In the present case, a well-defined strain gradient produces the desired force on the excitons.

The experiment is divided into two parts: the generation and calibration of an exciton energy gradient, and the actual measurement of the resulting exciton velocity. An ultrapure crystal of dislocation-free silicon ($N_A - N_D \lesssim 10^{12}$ cm$^{-3}$) was cut and etched to $1.5 \times 1.5 \times 4$ mm$^3$ dimensions with all $\langle 100 \rangle$ edges. A section of a 7.5-cm-diam steel ball bearing was pressed against the top of the sample as in Fig. 1(a). The crystal was cooled in a Janis Varitemp cryostat and excited by about 50 mW of $Ar^+$ laser light ($\lambda = 0.51$ $\mu$m). We left the excited area quite large (~300 $\mu$m across) to minimize the production of electron-hole droplets. Exciton recombination light was selected by a $\frac{1}{2}$-m spectrometer and detected by an infrared-sensitive photomultiplier tube.[7] A magnified image of the sample was scanned across the entrance slit of the spectrometer, allowing spatial scans with 30 $\mu$m resolution.

The technique we used to calibrate the force field eliminated any need for detailed knowledge of internal strains or deformation potentials. The excitation spot was positioned so that the excitons streaming toward the strain maximum moved along the [100] axis for about 400 $\mu$m [Fig. 1(a)]. As the image of the crystal was slowly scanned across the spectrometer entrance slit, a luminescence maximum defined the region where excitons of a selected energy were found. A series of such scans, Fig. 1(b), shows the increase in the recombination-photon wavelength as the excitons move into the crystal. The shift in the recombination energy as a function of distance into the crystal is plotted in Fig. 2. The

 

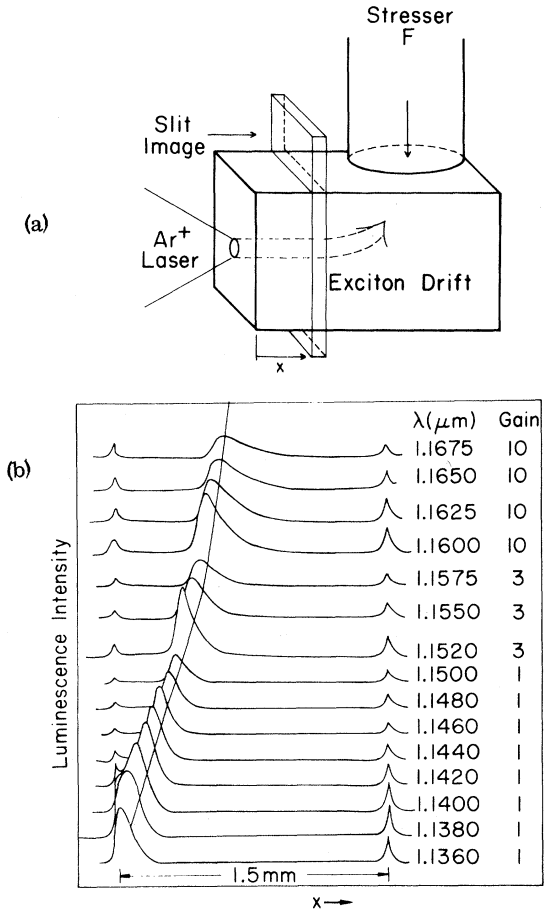


FIG. 1. (a) Configuration of the exciton drift experiment. The argon-laser light is absorbed within 1 $\mu$m of the crystal surface, producing excitons which drift into the region of maximum strain. (b) A series of spatial scans at 11 K with continuous laser excitation. The TO/LO-phonon–assisted exciton luminescence peak shifts continuously to longer wavelengths as the excitons move to regions of higher strain. The two smaller peaks are exciton luminescence scattered from the crystal edges.

force $\vec{F} = -\nabla U$ on the exciton was accurately determined and found to be nearly constant within 400 $\mu$m of the surface. An essential feature in these experiments is the ability to vary this force over a wide range, up to 0.5 eV/cm.

In the drift regime the momentum relaxation time $\tau$ is independent of applied force, and the drift velocity $v$ is given by

$$v = F\tau/m. \quad (1)$$

For motion along the [100] axis, the exciton mass is closely approximated by the sum of transverse masses of the electron and hole under [001] stress, $m_{et} + m_{ht} = 0.19m_0 + 0.26m_0 = 0.45m_0$. Typically the drift velocity is much less than the average thermal velocity of the free exciton $v_{th} = (3kT/m)^{1/2} = 1 \times 10^6 T^{1/2}$.

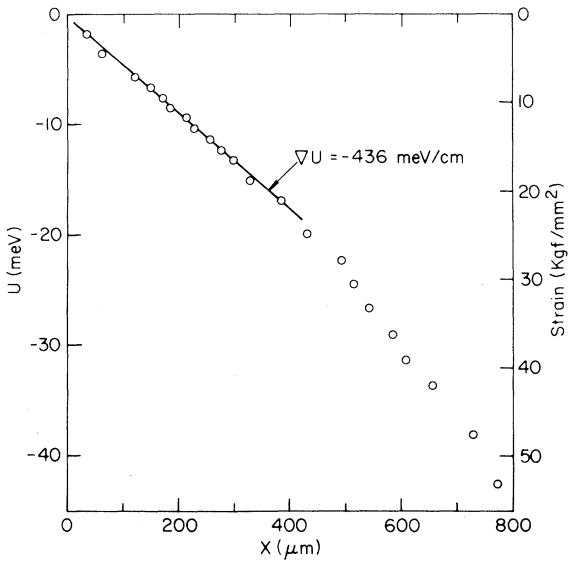


FIG. 2. The exciton energy gradient extracted from the slit scans of Fig. 1(b). The gradient, and therefore the force on each exciton, is found to be constant for 400 $\mu$m. The strain maximum was about 60 kg/mm$^2$ at $x = 830$ $\mu$m.

In the determination of the exciton velocity the laser was square-wave chopped at 20 kHz with a 200-ns rise time. An interval timer with 10-ns resolution recorded the delay between turnon and the detection of a luminescence photon by the photomultiplier tube. A histogram of the delay intervals was collected in a signal averager which displayed the signal buildup at a selected point in the crystal. The time shift of the buildup as a function of position $x$ yielded the local exciton velocity.

Figure 3 shows the exciton velocity measured at 11 K over a wide range of strains. At zero stress a finite velocity was observed which decreased with distance from the excitation surface and was attributed to exciton diffusion. A value of the exciton-diffusion coefficient, $D = 100 \pm 20$ cm$^2$/sec, was directly obtained from the time spreading of the signal buildup as a function of distance $x$. This was consistent with the value measured from the steady-state exciton distribution in the unstressed crystal as well as the zero-stress velocities shown in Fig. 3. As the stress was increased, the velocities grew linearly with the measured force, displaying a simple drift

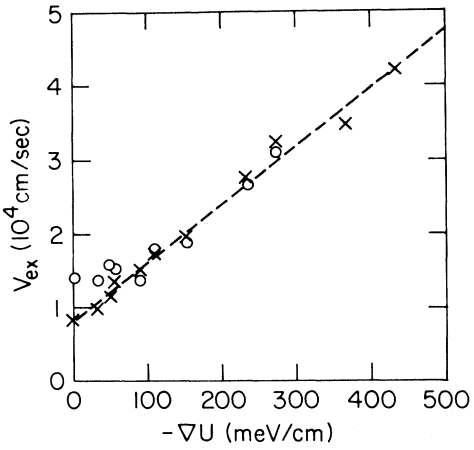


FIG. 3. The force dependence of the exciton velocity at 11 K. The circles indicate average velocities for $50\ \mu m < x < 150\ \mu m$. The crosses are average velocities measured between 50 and 400 $\mu$m into the sample. For $|\nabla U| > 100$ meV/cm the drift velocity is linear with the applied force and independent of position. The zero-strain velocity is due to exciton diffusion.

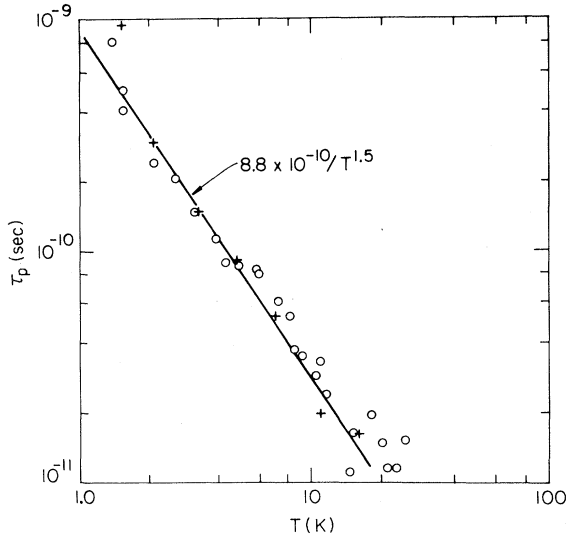


FIG. 4. The temperature dependence of the exciton-velocity damping time $\tau = mv/F$.

motion of the excitons in the induced field as in Eq. (1).

The momentum relaxation time was directly determined from the slope of the velocity-vs-force curve via Eq. (1). A complete force-velocity dependence was obtained at seven temperatures from 1.3 to 20 K; the resulting damping times are denoted by the plusses in Fig. 4. By measuring the velocity at high stress, and subtracting off the diffusion velocity, more data points were obtained, consistent with the more exacting measurements. A fit to all of the data yielded the result

$$\tau = [(8.8 \pm 0.5) \times 10^{-10}\ \text{sec} \cdot \text{K}^{3/2}]\, T^{-3/2}. \quad (2)$$

The simple acoustic-phonon scattering model[8] predicts

$$\tau_p = \frac{2\sqrt{2}}{3}\pi \frac{\rho s^2 h^4}{m^{3/2}E^2} \frac{1}{(kT)^{3/2}}. \quad (3)$$

For Si, with $m = 0.45\ m_0$, density $\rho = 2.3$ gm/cm$^3$, sound velocity $s = 5 \times 10^5$ cm/sec, and deformation potential $E \simeq 4$ eV,[9] this is evaluated as

$$\tau_p \simeq (10^{-9}\ \text{sec} \cdot \text{K}^{3/2})\, T^{-3/2}. \quad (4)$$

The data are consistent with both the predicted $T^{-3/2}$ dependence and the absolute magnitude of $\tau$. It is notable that the exciton drift relaxation time $\tau$ is about 4× shorter than the electron transverse relaxation time, $\tau_\perp = [(3.4\text{–}4.1) \times 10^{-9}\ \text{sec} \cdot \text{K}^{3/2}]$ $T^{-3/2}$, as determined from the cyclotron resonance linewidth.[10,11] At 1.3 K the equivalent charged-particle mobility of the exciton is $\mu_e = e\tau/m = (3 \times 10^6\ \text{cm}^2 \cdot \text{K}^{3/2}/\text{V} \cdot \text{sec})T^{-3/2} = 4 \times 10^6\ \text{cm}^2/\text{V} \cdot \text{sec}$.

The ability to measure simultaneously the drift and diffusion of excitons provides an opportunity to test the basic Einstein relation between diffusion coefficient and particle scattering time, $D = (\tau/m)kT$. From Eq. (2) one obtains $D = (300 \pm 20\ \text{cm}^2\ \text{K}^{1/2}/\text{sec})\text{T}^{-1/2}$. At 11 K, this predicts $D = 90$ cm$^2$/sec, in agreement with the independent measurement of $D$ given above. Measurement of $D$ from the steady-state spatial profile at zero stress is complicated by a wide variation in exciton lifetime at these temperatures.

This experiment demonstrates for the first time the use of calibrated strain gradients for carrier transport studies in indirect-gap semiconductors. It has confirmed a simple drift model for exciton transport in strained Si and determined the exciton momentum relaxation time. The results agree well with the acoustic-phonon scattering model over the range 1.3 to 20 K. There was no evidence of an upper limit to the scattering time, indicating that impurity scattering is unimportant for excitons in Si of such purity, even at these low temperatures. Further studies of less perfect material are indicated, to determine the form and magnitude of the scattering due to impurities or defects. The technique reported here should also be useful in characterizing the trans-

port of other photoexcited states in Si and Ge.

We wish to thank E. E. Haller for supplying the Si crystal, and M. W. Klein for the loan of the special photomultiplier tube. This project was supported by the National Science Foundation under the Materials Research Laboratory Grant DMR-77-23999, and by a Cottrell equipment grant.

[1]R. Haynes and W. Shockley, Phys. Rev. 75, 691L (1949). See also W. Shockley, *Holes and Electrons in Semiconductors* (Van Nostrand, New York, 1950).

[2]G. L. Pearson and J. Bardeen, Phys. Rev. 75, 865 (1949).

[3]P. P. Debye and E. M. Conwell, Phys. Rev. 93, 693 (1954).

[4]M. Costato and S. Scavo, Nuovo Cimento 54B, 169 (1968).

[5]R. S. Markiewicz, J. P. Wolfe, and C. D. Jeffries, Phys. Rev. B 15, 1988 (1977).

[6]P. L. Gourley and J. P. Wolfe, Phys. Rev. Lett. 40, 526 (1978).

[7]A. Varian, VPM-164 cooled to 200 K.

[8]J. M. Ziman, *Electrons and Phonons* (Oxford Univ. Press, Oxford, 1960), p. 433.

[9]As long as $\lambda_{ph} >> a_0$, where $a_0$ is the exciton Bohr radius, the exciton deformation potential is taken to be the shift in the band-gap energy with strain. This shift has been directly measured by I. Balslev, Phys. Rev. 143, 636 (1966).

[10]J. C. Hensel, Phys. Lett. 4, 38 (1963).

[11]E. Otsuka, T. Ohyama, and K. Murase, J. Phys. Soc. Jpn. 25, 729 (1968).

# Quantum Magnetic Hamiltonians with Remarkable Spectral Properties

Keith Miller[a] and Barry Simon[b]
*Department of Physics, Princeton University, Princeton, New Jersey 08544*
(Received 3 March 1980)

The Hamiltonian, $H$, of a spinless particle moving in two dimensions in an axially symmetric magnetic field $B(\rho)$ is considered. If $B(\rho) \sim \rho^{-\alpha}$ for $\rho$ large with $0 < \alpha < 1$, then it is shown that $H$ has spectrum $[0,\infty)$ with only eigenvectors and eigenvalues dense in $[0,\infty)$. If $\alpha = 1$, then the spectrum is a dense point spectrum in $[0,c]$ for suitable $c$ and absolutely continuous in $[c,\infty)$.

PACS numbers: 71.55.Jv, 71.30.+h

A subject of current interest is the study of quantum Hamiltonians describing electrons in random potentials. In terms of the spectrum, the conventional wisdom[1] is that in one dimension, $H$, after adding a suitable constant, will have the following properties (*Type I*): The allowed energy values (spectrum) are $[0,\infty)$ but there is a complete set of eigenvectors. This is accomplished by having eigenvalues $\lambda_n$ which are dense in $[0,\infty)$.

In more than one dimension, the expectation is *Type II*: The spectrum is still $[0,\infty)$. There is a number $d$ (the "mobility edge") with dense point spectrum in $[0,d]$ and with absolutely continuous spectrum in $[d,\infty)$.

Until one is used to it, these spectral properties are rather surprising, in part because one cannot write down an explicit "random" potential. For this reason, there may be some point in finding explicit Hamiltonians with these properties. We emphasize that no relation is claimed between the *physical reasons* for the spectral types found below and those in random systems. These results are, at this point, something of curiosities, but may have some relevance to physics in suitable magnetic fields. There also may be some point in studying transport at the mobility edge in these problems.

To begin with some explicit examples, let $\rho = (x^2+y^2)^{1/2}$. Then, the combination of operators

$$\left(\frac{1}{i}\frac{\partial}{\partial x}+\frac{cy}{(1+\rho)^\alpha}\right)^2+\left(\frac{1}{i}\frac{\partial}{\partial y}-\frac{cx}{(1+\rho)^\alpha}\right)^2 \qquad (1)$$

has type-I spectral properties[2] if $0 < \alpha < 1$, type-II with $d = c^2$ if $\alpha = 1$. For $\alpha > 1$, the spectrum is purely absolutely continuous.

The point of the proof of these properties is to note that (1) is the Hamiltonian of a spinless particle in two dimensions moving in a magnetic field, so that different spectral properties can be obtained by working in different gauges.

 